Identification of antisite carbon split-interstitial defects in 4*H*-SiC

J. W. Steeds and W. Sullivan
Department of Physics, University of Bristol, Tyndall Avenue, Bristol BS8 1TL, United Kingdom
(Received 29 June 2007; revised manuscript received 8 February 2008; published 9 May 2008)

A rich variety of optical centers with high energy local vibrational modes has been found in electron-irradiated 4*H*-SiC in both the as-irradiated and annealed states. These energies have been measured and the annealing dependence of the optical centers has been investigated by low-temperature photoluminescence spectroscopy. In view of the relatively high energies of these modes, it is anticipated that they involve carbon interstitials and a detailed correlation has therefore been undertaken, in selected cases, between the experimentally observed energies and those calculated by recent local density approximation, i.e., *ab initio* methods for atomic arrangements involving carbon interstitials. When satisfactory agreement has been achieved, the annealing behavior is compared to the calculated stabilities of the defects concerned. As a result, different configurations of carbon antisite defects are identified together with their spatial distributions with respect to the irradiated areas and their sequences of appearance and disappearance on annealing. These findings significantly add to the understanding of the radiation damage process and its subsequent development and recovery on annealing. Some of the optical centers that have well-defined local vibrational modes remain to be identified in the future.

DOI: 10.1103/PhysRevB.77.195204 PACS number(s): 61.72.J−, 61.80.Fe, 63.20.Pw, 81.05.Hd

I. INTRODUCTION

The nature of defects introduced into 4*H*-SiC during growth or by atomic displacements caused by high energy electron irradiation, by ion implantation, or by other processing steps is of both practical and fundamental importance. As impressive progress is being made in understanding the nature and experimental signatures of intrinsic defects in 4*H*-SiC, this material may represent well a unique opportunity to arrive at really detailed knowledge of the atomic processes that occur in a compound semiconductor during growth, irradiation, implantation, and annealing. This is a consequence of the wide band gap that accommodates a great variety of deep levels, such as the considerable number of sharp zero phonon lines (ZPLs) in low-temperature photoluminescence (PL) spectroscopy and of the sharp lines in electron paramagnetic resonance (EPR) spectroscopy. The carrier diffusion lengths are typically ≤ 5 μm so that excitation does not diffuse far from its origin. The unit cell is small enough to permit accurate *ab initio* calculations and, as it contains two sublattices, issues such as stoichiometry and antisite defects are important. The lessons being learned from this material may well have much wider application to other compound semiconductors that lack the combination of properties exhibited by 4*H*-SiC. Recent work has produced good understanding of vacancy-related defects and their complexes, although uncertainties remain. In particular, EPR studies have identified V_c^+ (Umeda *et al.*[1]), V_c^- (Umeda *et al.*[2]), V_{Si}^- (Mizuochi *et al.*[3]), nearest neighbor (V_cV_{Si}) pairs (Son *et al.*[4]), and $(V_cC_{\mathrm{Si}})^-$ (Umeda *et al.*[5]) and $(V_cC_{\mathrm{Si}})^+$ (Umeda *et al.*[6]) pairs, although the correlation for V_{Si} containing centers between PL experiments and the results of EPR and related techniques is still under investigation (Mizuochi *et al.*[7]).

Self-interstitials are less well understood, although it is generally accepted that they are more mobile than the vacancies, i.e., carbon interstitials being particularly mobile, and so they often are an important route for vacancy elimination (Bockstedte *et al.*[8]). At present, the deep centers responsible for degradation of the electrical properties of 4*H*-SiC have generally been associated with vacancy-related defects,[9] but as these are the only defects currently identified, this situation may change when the interstitial-related defects are better understood.[10] In fact, recent work (Grossner *et al.*[11]) indicates that the prominent deep traps $Z_{1/2}$, which are identified by deep level transient spectroscopy, are related to complex defects involving carbon interstitials. They are important for other reasons since they are potential sources of internal stress and, when the complexes grow large enough, they can nucleate dislocation loops.

This work is concerned with carbon interstitial-related defects. There have been a number of recent detailed *ab initio* calculations for possible configurations of such defects[12,13] but, up until now, they have lacked any secure experimental verification. Here, we provide a large body of experimental data that can be compared to detail with the results of the calculations. Since the insertion of additional atoms into the lattice causes local stiffening, it is to be expected that optical centers involving them will have local vibrational modes (LVMs), and in the case of the lighter C atoms, modes are of quite high energy. As the calculations involve the ground states of defects, photoluminescence spectroscopy, with vibronic structures related to the ground states of the defects, offers an obvious route to investigate the formation of centers that match the available data. The present publication, together with a closely related work (Steeds *et al.*[14]), is devoted to this exercise.

After giving the experimental details, we discuss the methods that have been used to associate a given spectrum with an individual defect and then summarize the results obtained in this way. A few of these centers have been mentioned in previous reports, most have not. We then embark on an attempt at correlating our results with the *ab initio* calculations. Some of these optical centers can be matched quite well with the calculated LVM energies and stabilities

and we concentrate on these. One aspect of this work involves a triplet of ZPLs with wavelengths close to 463 nm. Their behavior under optical excitation is quite remarkable and, as has been investigated in some detail, it is separately treated in the associated publication (Steeds *et al.*[14]). Finally, the outcome of the attempted correlations is summarized and some implications for other studies of defects in 4*H*-SiC are addressed.

II. EXPERIMENTAL DETAILS

Most of the samples studied during the course of this investigation were irradiated at room temperature by using the pure (ion-free), highly monochromatic, electron source of a transmission electron microscope (TEM) (Philips EM 430). The irradiations were locally performed on bulk specimens with an electron beam of circular cross section having a diameter of either 100 or 200 μm and a uniform intensity distribution with a sharp cutoff at the perimeter. The electron energy was normally 300 keV, but lower energy irradiations were also performed, which are mostly at 250 keV, and only a small number of irradiations at energies below that. Electron doses covered a wide range from 10^{17} to 2×10^{20} e cm^{-2}, but most of the results discussed here came from samples irradiated with doses greater than 10^{19} e cm^{-2}. For higher energy irradiations, which were up to 1 MeV, high voltage TEMs at the Max Planck Institute in Stuttgart and at the Lawrence Berkeley Laboratory in California were used.

After irradiation, the samples were studied by low-temperature PL microscopy by using Renishaw micro-Raman systems fitted with the Oxford Instruments cryogenic stages. One of these Renishaw systems was operated with a 325 nm He/Cd laser; the other used an argon-ion laser that was normally operated at 488 nm, but experiments were also performed with 457.9 nm excitation. For the 325 nm operation, the laser spot size was approximately 5 μm in diameter with 3 mW of power at 100% operation (it was generally operated at 1% or 10%). For the 488 nm laser, the power level was <10 mW, which is focused into a 3 μm spot. Three different modes of operation were commonly used. These were the spot mode, with the laser incident at a chosen location on the sample, the line-scan mode, where spectra were collected at equally spaced points (typically 10 or 20 μm apart) along a chosen line, and the mapping mode, where the spectra were collected at a rectangular array of points. The sample temperature for most of the experiments was approximately 7 K, except when the temperature dependence of emission was being investigated. Time-dependent experiments were performed on a separate system fitted with an acousto-optical modulator and a GaAs photocathode. Isochronal annealing was performed on several of the samples with an annealing time of 30 min. Initially, the samples were annealed with 100° increments, but in critical temperature ranges, annealing intervals of 50° were used. The annealing carried out at temperatures above 1000 °C was performed in a specially designed furnace.[15]

The samples studied were obtained from nine different sources, which are mostly in the form of thick (30 μm-100 μm) n(N) and p(Al) doped epitaxial layers, with doping concentrations varying from $10^{14}\times10^{17}$ to 6×10^{17} cm^{-3}. Material suppliers included the Institute for Crystal Growth, Berlin (G Wagner), the University of Linköping (P Bergman), Cree, SiCED (P Friedrichs), and CNR-IMM Catania (F LaVia). Altogether, many thousands of spectra have been produced and studied to provide the data presented here.

III. METHODOLOGY USED

Photoluminescence spectroscopy of electron-irradiated 4*H*-SiC generally reveals a wealth of experimental detail that has to be broken down into specific spectra that are associated with individual defects. A number of different methods have been used in this work to achieve the deconvolution. Since all the data were obtained by local irradiation by using a TEM, one simple method used was to investigate the spatial distribution, both within and outside the irradiated regions, by looking for spatial correlations. It is a common characteristic of centers with high energy LVMs that higher harmonics exist and their regular correlation with specific ZPLs in the thus separated spectra is therefore a good indication that effective deconvolution has been achieved. However, there are several other techniques that have been employed. One involves an investigation of the temperature at which the spectra of interest appear and then disappear on annealing. Others involve determination of the electron dose or the accelerating voltage required to create the spectra. Finally, the spectra can be studied by using different excitation wavelengths (325 and 488 nm have been most frequently used in this investigation) or different sample temperatures. If a particular spectrum under study is present under different excitation conditions, it should have similar spectral characteristics, although its intensity relative to other spectral details is often very different. The requirement that all the elements of a particular spectrum should remain in a fixed relationship is a very stringent one. Cases where the process of deconvolution is incomplete are not included in this work.

IV. EXPERIMENTAL RESULTS AND COMPARISON TO CALCULATIONS

Before embarking on the exercise of comparison between experiment and theory, it should be pointed out that the theoretical work is largely based on relatively small defect clusters. Even for dicarbon, interstitials on a carbon site at least six different atomic arrangements exist. Dicarbon antisite pairs and a tricarbon antisite have also been investigated, but clearly the number of possible configurations greatly increases as the number of C atoms involved increases. The experimental situation is, however, rather different, with lower energy configurations being chosen on the basis of ease of formation or the size of energy reduction rather than on the number of C atoms in the center. Of course, the ability to form large clusters could be limited by the probability of the number of atoms required to come into close proximity. However, the experimental evidence is that C interstitials are extremely mobile under the conditions of electron irradiation

TABLE I. Experimental results for common optical centers having local vibrational modes in electron-irradiated 4*H*-SiC. The two columns at the left side define the wavelength and energy of the zero phonon line of the center. The LVM values are given with an accuracy of ±0.1 meV.

Wavelength of ZPL (nm)	Energy of ZPL (eV)	Gap modes (meV)	Other LVMs (meV)	Highest energy LVM (meV)
414.2	2.992		119.9, 122.5	129.2
450.6	2.751	74.8	135.1	180.0
456.7	2.714			133.5
463.3	2.675		132.8	179.8
463.6	2.674		132.5	178.5
464.3	2.670		131.9	180.0
465.7	2.662			177.8
471.8	2.627		151.8, 189.4	246.9
493.5	2.512		166.85	169.8
498.5	2.487			179.9
520.6	2.381		122.1	172.3
596.8	2.077	83.1	123.9	149.1
599.3	2.068	77.3, 79.2, 83.0, 87.9	124.4, 160.5	180.5

so that complex configurations might form. One can therefore expect that the measure of agreement will be limited. However, the accuracy with which the calculations of LVMs can be performed is rather good and errors of less than 10 meV are claimed by the authors.[12,13]

A summary of several of the common optical centers that have been found to have LVMs is given in Table I, which includes the LVM energies observed. In particular, it includes the centers studied in some detail here as well as others having high energy LVMs around 180 meV, which are similar to those of the dicarbon antisites that are the subject of the associated paper.[13] These results are given here; those for the triplet of lines at 463 nm were the subject of a preliminary discussion[16] and the ZPL at 414.2 nm that was previously referred to as HT2.[17] Table I includes centers that have different spatial distributions and different temperature ranges over which they were observed. An overview of the annealing dependence of the PL intensities of different ZPLs is given in Fig. 1. The results in Fig. 1 were obtained for one particular specimen [Al doped, N_A-N_D $(7.0\times10^{15}$ cm$^{-3})$, without donor-acceptor pair emission, with thickness of 36.4 μm, with dose of 10^{20} e cm^{-2}] and, although they are generally representative of other samples subjected to a similar electron dose, the details were found to vary somewhat from one sample to another and to considerably vary with change in dose. The figure also includes, for reference purposes, data for other commonly observed and intense ZPLs such as the *a*-*d* alphabet lines,[18] V_1,[19] and D_I (Ref. 18) luminescence. It has results for 488 and 325 nm excitation. A few of the ZPLs could be observed with both laser excitations. Table I also includes results from centers for which the PL intensity was concentrated within the irradiated region as

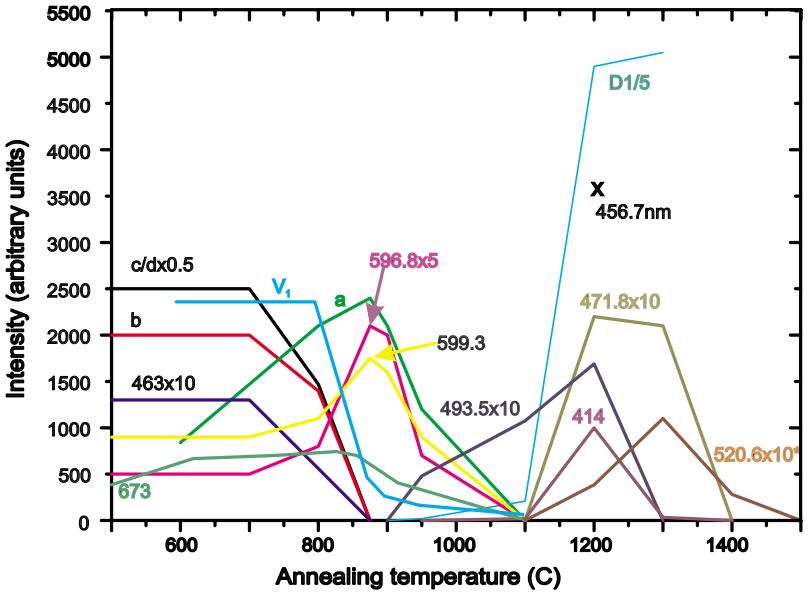

FIG. 1. (Color online) Dependence of the ZPLs in Table I on annealing for one particular sample [Al doped, N_A-N_D $(7.0\times10^{15}$ cm$^{-3})$, without donor-acceptor pair emission, with thickness of 36.4 μm, with dose of 10^{20} e cm^{-2}]. Extra lines added include the alphabet lines *a*-*d*, the Si vacancy (V_1), and the 673 nm ZPL. The *x* on the 520.6 nm ZPL indicates that the result comes from a different sample. Results were obtained by using both 325 nm and 488 nm excitation. The graphs have been scaled as indicated. The PL results were obtained at a sample temperature of ~7 K.

well as those found outside it. The principal lines predominantly outside the irradiated area under 325 nm excitation were the *b*-*d* alphabet lines and the 463 nm triplet. Note that where an optical center appears by up-conversion in Fig. 1, its disappearance above a certain temperature might only indicate the loss of the up-conversion mechanism.[14] A comparison between the observed and calculated LVM energies provides some encouraging agreements and we shall concentrate on these here by placing the greatest emphasis on the highest energy modes. The highest energy modes are preferred for a more fundamental reason. It is unlikely that any of the local vibrational modes will have well-defined symmetry in view of the complexity of the centers and the relatively low symmetry of 4*H*-SiC. In addition, there is insufficient knowledge of the excited states of interest to allow the prediction of which modes would be excited even if the mode symmetries were well defined. However, one good generalization is that the highest energy modes will be symmetric stretching modes and therefore most likely to appear in PL experiments.

A. Optical centers with a highest energy local vibrational mode of about 180 meV

The most complete comparison between theory and experiment has been made for the triplet of three ZPLs labeled 463 (nm) on Fig. 1. As shown by Steeds *et al.*,[14] this triplet can be interpreted as coming from four ZPLs (two of them unresolved in our experiments) and having their origin in dicarbon antisites, that is, two carbon atoms sitting on a Si site. These four ZPLs are related to defects on the pseudohexagonal and pseudocubic sites having either spin $S=0$ or $S=1$. Although they disappear from the 488 nm spectra above 900 °C, it is not certain that they anneal out at this temperature because of the up-conversion process involved in their excitation. However, the change in relative and absolute intensities of the individual lines of the triplet for temperature increases up to 900 °C and the fact that up-conversion is preserved for several other optical centers above 900 °C, including D_I, up to, probably indicates that a change in atomic configuration has occurred. Quite different behavior is found under 325 nm excitation as described by Steeds *et al.*,[14] and with this excitation wavelength, the 463 nm triplet can certainly be observed at higher temperatures up to 1300 °C as will be discussed.

At first sight, the many centers with 180 meV LVMs (Table I) might all be thought to be candidates for the dicarbon antisite defects. Even though the evidence presented[14] may be regarded as convincing, it is important to demonstrate that other centers exist with somewhat similar properties in view of the discussion that has occurred about the five *P*-*T* centers in 6*H*-SiC.[20] Each of the additional ZPLs detected in these experiments was apparently distinct with different properties. The most obvious parallel exists for the optical center with its ZPL at 450.6 nm (Table I). This also has a lower energy LVM at 135.1 meV, which is in good agreement with the calculated energies for the dicarbon antisite.[12] However, the dicarbon antisites have been identified; there is only one other center for which similar LVM energies have been calculated. This occurs in the recent work of Eberlein *et al.*[20] where they found energies of 140 and 177 meV for the recombination of an electron trapped on a dicarbon antisite with a hole trapped on a nearby silicon antisite. The 450.6 nm center was not normally found in the as-irradiated state but it annealed in at temperatures above 500 °C and persisted up to 1200 °C so that it is apparently somewhat more stable than the 463 nm triplet. In fact, it has rather similar properties to those of the P center in 6*H*-SiC. The center did not exhibit the metastability of the 463 nm triplet under intense 325 nm exposure. These properties make a connection with the center of Eberlein *et al.*[20] problematical. None of the remaining four optical centers (ZPLs at 465.7, 498.5, 520.6, and 599.3 nm) have additional LVMs at the lower energy of about 130 meV (Table I). The center at 599.3 meV has additional LVMs that do not match the calculations for the dicarbon antisite[12] but are, however, in reasonably close agreement with the calculated energies for one of the carbon di-interstitial configurations.[12] The LVM energies for the even modes of the configuration, which are designated as $(C_{sp})_{2,hk,\mathrm{cub}}$, are given as 189.1 and 161.3 meV.[21] These vary from the experimental values by a larger margin than is the case for carbon antisite defects, but the difference is still within the range of uncertainty of the calculations. This defect is calculated to have dissociation energy of 5.5 eV, which is consistent with the observed high thermal stability (Fig. 1). The other three centers were all produced by high-temperature anneals. The 465.7 and 498.5 nm centers were found in the temperature range of 950–1300 °C, while the 520.6 nm center had an even higher-temperature range of existence (see Fig. 1) and an LVM of significantly lower energy than the dicarbon antisite. The 498.5 nm had an intense and sharp LVM with second and third harmonics clearly visible and was concentrated in the irradiated region. It was observed with both 325 and 488 nm excitations. The 465.7 nm center was only observed with 325 nm excitation, and it had a broad intensity distribution extending well outside the irradiated region. Its intensity was enhanced on exposure to an intense 325 nm beam.

B. Tricarbon antisite

The center with a ZPL at 471.8 nm appeared on annealing to 1200/1300 °C. It is of particular interest because of the quite remarkably high LVM energy of 246.9 meV. The spectrum of this center is shown in Fig. 2 where the high energy LVM is labeled LM3 to distinguish it from two other considerably weaker LVMs of lower energy (LM1 and LM2). These LVMs also appear in second order (2LM1, 2LM2, and 2LM3). The only previous experimental record of such high energy LVMs in SiC was in the case of the 6*H* polytype[22] and this result was recently interpreted[21] as a particular configuration of a tricarbon antisite and three carbon atoms on a Si site, where two of them are very close together and acting effectively as dicarbon molecule as far as the stretch mode was concerned. At the time of this publication, the only experimental results available were for 6*H*-SiC although the calculations were performed for 4*H*-SiC. The present experimental results, for the 4*H*-SiC polytype, were obtained under

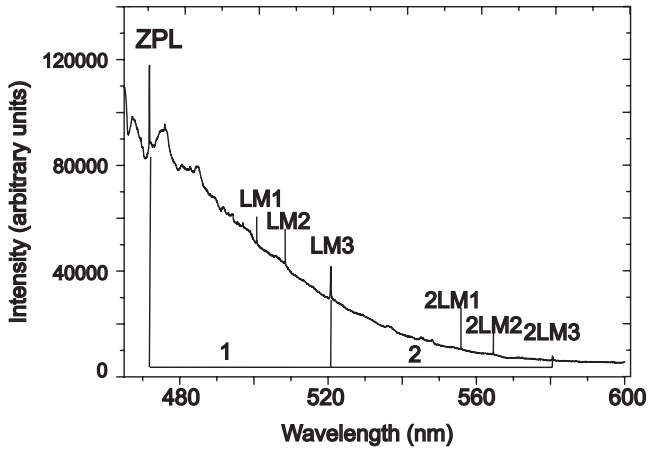

FIG. 2. Spectrum of the tricarbon antisite defect in 4*H*-SiC. The three LVMs (LM1, LM2, and LM3) are repeated as sum modes in the second order spectrum (2). It was acquired at ~7 K by using 325 nm laser excitation.

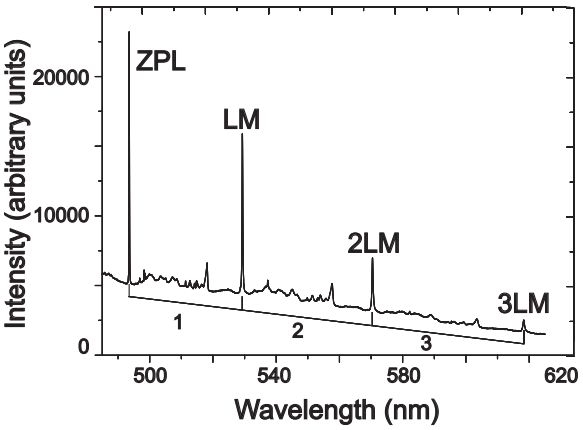

FIG. 3. Spectrum of the 493.5 nm center interpreted here as the $kh_{,\mathrm{hex}}$ dicarbon antisite pair in 4*H*-SiC. In this case, the coupling is so strong that two orders of sum modes are clearly visible as indicated by the numbers below the curve. The spectrum was acquired at ~7 K by using 325 nm laser excitation.

similar circumstances to those for the 6*H*-SiC specimens but are now for the actual polytype for which the calculations were performed. The calculations arrived at slightly different energies for the LVMs when the defect sits on the pseudohexagonal or the pseudocubic site, which is the largest difference occurring for the highest energy LVM (255.7 meV compared to 254.9 meV). These differences are probably below the resolution of the present experiments if the two ZPLs are similarly close in energy because the linewidth of the relevant LVM was 1 meV (full width half maximum). Further, the calculations are not accurate to 1 meV and they are unable to predict the energies of the ZPLs. The results of a comparison between theory and experiment are shown in Table II and reasonable agreement is demonstrated for the three observed LVMs. We therefore conclude that the 471.8 nm center is related to the tricarbon antisite. As supporting evidence for this conclusion, the calculated thermal stability of this center is 5.8 eV, which is in reasonable accord with experiment

C. The dicarbon antisite pair

We next consider the center with its ZPL at 493.5 nm. This center becomes quite strong after annealing room-temperature-irradiated samples in the range of 850–1200 °C, but it is not found outside this range. It has a characteristic appearance (Fig. 3) with intense first, second, and third order LVM emissions. It is predominantly polarized with **E** parallel to [0001]. Its LVM energy of 169.8 meV is a reasonable match with one of the many possible configurations for dicarbon antisite pairs. This particular configuration involves pseudocubic and pseudohexagonal sites and lies within the hexagonal plane and has a LVM energy of 172.0 meV (Ref. 23) (see Table II). Here, it is designated as $kh_{,\mathrm{hex}}$. However, the calculations indicate that the various configurations of the dicarbon antisite pair (seven have been studied) have a property not shared with any of the other defects involving carbon interstitials so far investigated (of which there are about another 12); they have another high energy LVM.[12] At first, this special property was not experimentally detected, but a small number (5) of very high quality spectra, without spectral overlaps, were obtained with long acquisition times and in every case an additional weak peak was observed on the short wavelength side (lower LVM energy) of the highest energy LVM (see Fig. 4). By peak fitting, this additional peak was found to correspond to a LVM energy of 166.9 meV. This energy is not only in reasonable agreement with the calculation but is also lower than the highest energy mode by 2.9 meV, which is in excellent agreement with the calculated difference (Table II). Additional information comes from the annealing behavior of the center. As can be seen from Fig. 1, the 493.5 nm ZPL appears as the 463 nm triplet vanishes under 488 nm excitation and itself anneals out when the 471.8 nm center anneals in.

TABLE II. Calculated and experimental LVM energies for $(C_3)_{\mathrm{Si}}$ (k site) and $[(C_2)_{\mathrm{Si}}]_{2,kh,\mathrm{hex}}$. The values were taken from Ref. 12.

LVM energies (meV)	Theory (meV)	Experiment (meV)	Calculated dissociation energy (eV)
$(C_3)_{\mathrm{Si}}$ (k site)	154.0, 182.3, 254.9	151.8, 189.4, 246.9	5.8
$(C_3)_{\mathrm{Si}}$ (h site)	154.2, 182.6, 255.7		
$[(C_2)_{\mathrm{Si}}]_{2,kh,\mathrm{hex}}$	169.1, 172.0	166.85, 169.8	6.7

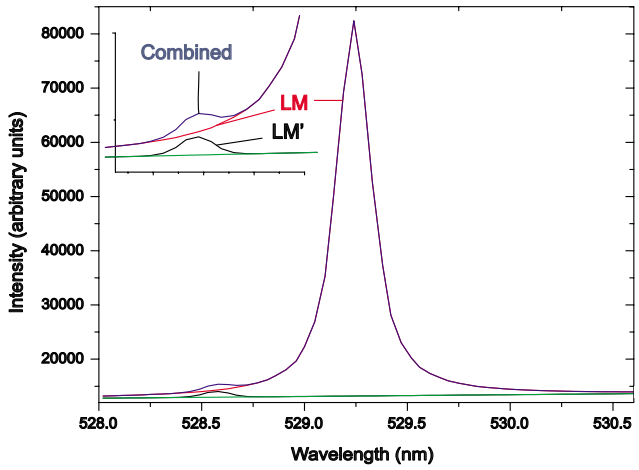

FIG. 4. (Color online) Detail of the LM local mode of the 493.5 nm center illustrated in Fig. 5. Deconvolution of the spectrum has been performed, as shown in the inset, to determine the energy of the considerably weaker side band (LM') on the short wavelength side of LM. The spectrum was acquired over 15 min at ~7 K by using 325 nm laser excitation.

D. Spatial distributions of intensity

Emphasis has been placed in this work on the observed intensity distributions with respect to the irradiated regions. As mentioned earlier (Sec. III), this played an important part in the deconvolution of overlapping spectral systems. Two further aspects of the intensity distributions could also have a bearing on the defect identifications discussed here. As this activity is not well known (or well understood), some preliminary remarks are called for. Very different spatial distributions have been frequently encountered in this investigation. They are strongly dependent on the electron doses applied. Extremes of behavior are exhibited by some of the alphabet lines as compared to the D_I luminescence. Figure 5

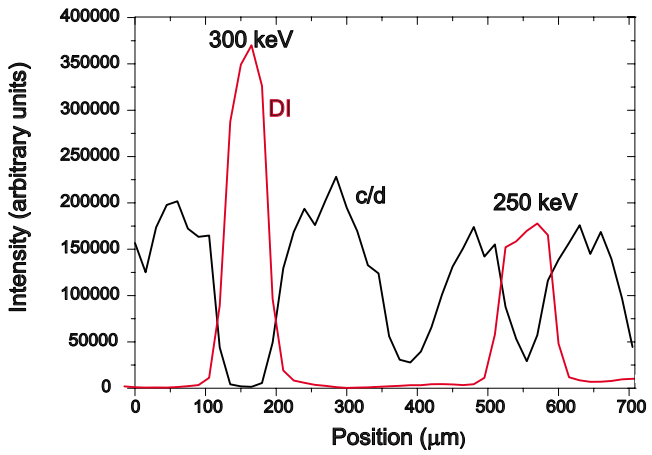

FIG. 5. (Color online) Line scans of PL intensity variations across two 100 μm diameter electron-irradiated areas of a sample. The c/d spectra were acquired after a 300 °C anneal and the D_I spectrum was acquired from the same region after a 1200 °C anneal. The spectra were obtained at ~7 K by using 325 nm laser excitation.

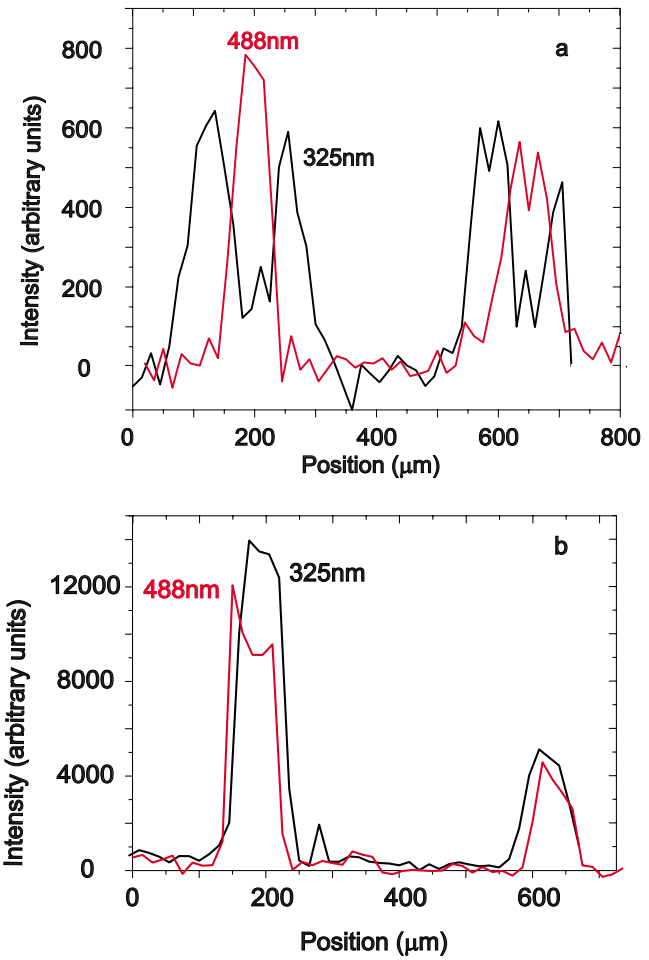

FIG. 6. (Color online) Figures comparing the ZPL integrated intensity distributions across two 100 μm diameter irradiated areas observed for different optical centers by using 325 and 488 nm laser excitations at ~7 K. The irradiations on the left side of the figures were performed at 300 keV, on the right at 250 keV; the dose was 10^{20} e cm^{-2} in each case. (a) ZPL of 450.6 nm for a sample annealed to 1100 °C; note the drop off of intensity in the irradiated region and the spread of intensity outside it for 325 nm excitation. (b) ZPL of 471.8 nm for a sample annealed at 1200 °C; note the similarity of the results at the two wavelengths.

shows the intensity distribution of the c/d alphabet lines in an as-irradiated sample compared to that of the D_I center after annealing at 1300 °C. These results are for a dose of 10^{20} e cm^{-2} at 300 keV. More important is the observation that the intensity distributions for a given sample with different excitation wavelengths may be quite different. One such example is that of the 463 nm triplet discussed in the associated paper.[14] Less complicated behavior is that of the 450.6 nm center [Fig. 6(a)]. This result, for a sample irradiated to a dose of 10^{20} e cm^{-2} at 300 and 250 keV and subsequently annealed at 1100 °C, showed quite different intensity distributions at 325 and 488 nm. The difference between them is likely to be the result of different excitation processes in the two regions with up-conversion at 488 nm dependent on other defects that do not exist outside the irradiated area, while the above-band-gap excitation could ionize these defects. The 488 nm intensity for this sample reached its maxi-

mum value after an 800 °C anneal, whereas the 325 nm intensity was a maximum after a 1100 °C anneal when the competitive excitation of intense emission from the alphabet lines was eliminated. Further, the actual form of the intensity distributions changed with annealing, with the 325 nm results having a narrower width as they shortly increased in intensity before annealing out. The intensity distributions observed for the 493.5 nm center under 488 nm excitation were similar to those for the 450.6 nm center, even though upconversion was no longer required, but the 325 nm distributions, while very broad, lacked the central dip of intensity of the 450.6 nm center. The experimental evidence of intensity continuity across the gap caused by the holographic notch filter[14] indicates that the excitation process for below-band-gap excitation is the same for laser wavelengths above and below the notch. In each case, the maximum intensities of emission at the two different wavelengths occurred after anneals at about 100 °C higher than for the 450.6 nm center. By way of contrast, the intensity profiles for the 471.8 nm center are very similar for both 325 and 488 nm excitations [Fig. 6(b)].

Bearing in mind the obvious limitations of the method, it is, nevertheless, of interest to enquire whether the observed distributions offer support for the progression from carbon antisites to pairs of antisites and then to tricarbon antisites as suggested by the annealing curves in Fig. 1. One might expect that the spatial distributions of one center transforming into another would be similar. When 488 nm excitation was used, similar spatial distributions were observed for each of the three centers (463 nm triplet, 493.5 and 471.8 nm ZPLs). However, the situation is more complicated for 325 nm excitation for several reasons. The 463 nm triplet was created by exposure to the beam, the 493.5 nm center had a rather broad distribution, but the 471.8 nm center was limited to the irradiated region.

An alternative way of making use of the intensity distributions is suggested by the observation[14] that the 463 nm triplet can be created by an intense 325 nm beam in samples annealed at 1300 °C. Does this come about by release of a carbon interstitial from the tricarbon antisite or the dicarbon antisite pair? There is some evidence to support this idea [Fig. 7(a)]. A technique described in the associated paper was used. It involves scanning the 325 nm beam along a line through the electron-irradiated region and subsequently investigating the modified intensity distributions by creating spectra at much lower laser power (1%). Figure 7(a) shows the intensity distributions of the three relevant ZPLs across this line for a sample annealed at 1300 °C. To minimize the effects of specimen drift, the collection time of the individual spectra from which these intensity profiles were derived were obtained was only 10 s. The enhancement of 463 nm triplet intensity is correlated with reduction in intensity of the two other centers. A similar experiment was carried out on another sample after annealing at 1100 °C [Fig. 7(b)]. At this temperature, the 496 nm triplet has annealed out and the 493.5 nm center has created. Once again, the creation of 463 nm triplet intensity is correlated with loss of the 493.5 nm center. However, more extensive investigation, involving mapping the relevant areas, revealed that these results only occurred in a narrow spatial range near the periphery of the

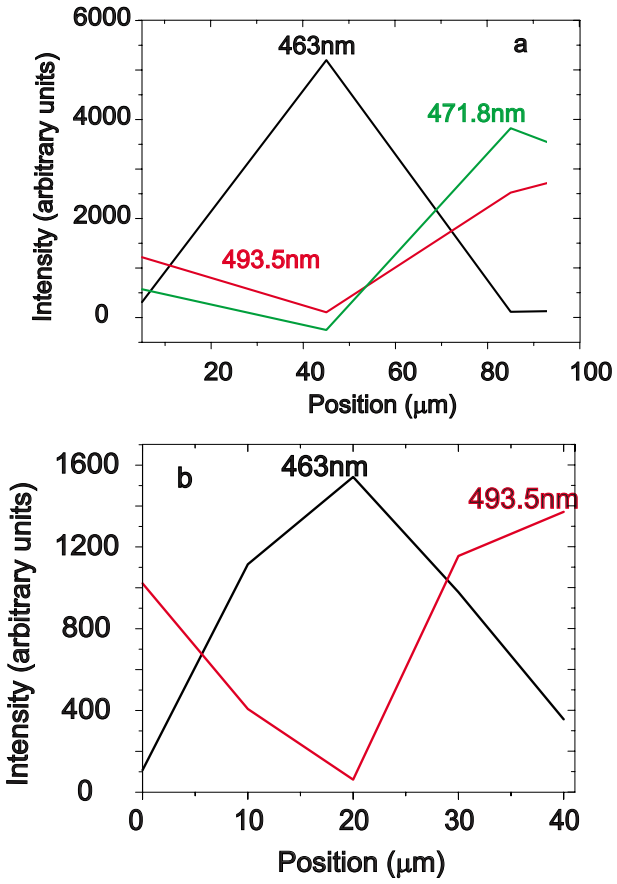

FIG. 7. (Color online) Figures illustrating the changes in integrated intensity of specified ZPLs as a consequence of exposure to an intense 325 nm beam at ~7 K. The results come from the periphery of the irradiated regions and the intensity profiles were obtained by using the low-power (25 times reduction) 325 nm excitation ~7 K along a line perpendicular to the linear trajectory of the intense 325 nm beam. (a) Enhancement of 463 nm intensity and reduction of 471.8 and 493.5 nm intensities for a sample annealed at 1300 °C. (b) Enhancement of 463 nm intensity and reduction of 493.5 nm intensity for a sample annealed at 1000 °C.

irradiated areas. Further, outside the intensity of the 463 nm triplet increased in regions where neither of the ZPLs of the other two centers existed. Moreover, it cannot be ruled out that the results in Fig. 5 might be the consequence of competition between the centers for the excitation injected. In any case, the majority of the 463 nm triplet centers were created from defects that do not appear in the spectroscopy performed in these experiments.

V. DISCUSSION OF RESULTS

A detailed comparison between the calculated properties, particularly the energies of the LVMs of C interstitial-related defects, and the experimental results reported here, for optical centers in irradiated and annealed 4*H*-SiC, has produced several examples of close agreement. Of particular interest is the annealing sequence of the identified defects which, in fact, all involve C antisites. The dicarbon antisite defects are created in the as-irradiated state. They can also be created

from other defects by exposure to an intense 325 nm laser beam. They exist in two spin states and the $S=1$ defects should therefore be detectable in EPR experiments but have not yet been reported. At a temperature of about 900 °C, there is evidence that these defects anneal out and that they are replaced by a particular configuration of a pair of dicarbon antisites. At higher temperatures, still the dicarbon antisite pairs are replaced by a tricarbon antisite defect that is particularly thermally stable and has a very high energy LVM. The results obtained suggest that this process of aggregation may be to some extent reversible under the influence of an intense 325 nm laser beam, which convert the tricarbon antisite and the dicarbon antisite back into a dicarbon antisites. The tricarbon antisite and the dicarbon antisite are stable to relatively high annealing temperatures (1100–1300 °C), and, once eliminated, only the well-known D_I and D_{II} centers remain in PL spectra. These results represent the first clear experimental evidence of the existence of carbon antisite defects in electron-irradiated 4*H*-SiC. They suggest that carbon antisite defects may be involved in the D_I and D_{II} centers that replace them, as is often asserted (Mattausch *et al.*[24] and Gali *et al.*[13]). The appearance of thermally stable D_{II} luminescence in 750 °C irradiated 4*H*-SiC indicates that high-temperature irradiation may have unwelcome consequences. The failure to identify, at present, C interstitial-related complexes on C sites is another interesting outcome of this investigation.

A by-product of the results presented here apparently challenges the interpretation of the *a-d* alphabet lines as nearest neighbor C_{Si}-Si_C pairs that convert to D_I centers at higher temperatures.[20] First, although the $b-d$ lines anneal together, the annealing of the a line is quite different. Second, there is a 400 °C temperature interval between the annealing out of the $b-d$ lines and the annealing in of the D_I center. Finally, the spatial distributions of the $b-d$ centers are quite different from that of the D_I center since the former are concentrated outside the irradiated region while the latter is concentrated within it.

There remain several optical centers that were observed in this work for which no link could be found to the calculated LVM energies. Two of these have relatively low energy LVMs and might therefore be related to Si interstitial complexes. C-Si complexes may also exist and have higher energy LVMs. Future calculations could help us to clarify the situation. In addition, there are numerous possibilities of more complex aggregates, including C aggregates, that have not yet been the subject of *ab initio* calculations. None of the defects studied here has sufficient thermal stability to account for the $Z_{1/2}$ or the $EH_{6/7}$ defects well known[9,25] from deep level transient spectroscopy measurements and believed to be important in controlling the electrical properties of 4*H*-SiC.

VI. SUMMARY AND CONCLUSIONS

A detailed comparison to experimental results obtained by low-temperature PL microspectroscopy of electron-irradiated 4*H*-SiC with calculated LVM energies of C interstitial clusters has produced a number of successful correlations. Nevertheless, a considerable number of the experimental centers remain without credible atomic models at present. The centers that have been identified with a reasonable level of confidence all involve carbon antisite defects. The dicarbon antisite is found in the as-irradiated state after room-temperature irradiation to an electron dose of $\geq 5 \times 10^{19}$ cm^{-2}. As it anneals, first (at 850 °C) dicarbon antisite pairs, and then, at a slightly higher temperature (1000 °C), tricarbon antisite defects are created.

ACKNOWLEDGMENTS

The authors would like to thank the UK Science and Engineering Research Council for partial support of this work and N. G. Wright of the University of Newcastle for high-temperature sample annealing above 1100 °C.

[1] T. Umeda, J. Isoya, N. Morishita, T. Ohshima, and T. Kamiya, Phys. Rev. B **69**, 121201(R) (2004).
[2] T. Umeda, Y. Ishitsuka, J. Isoya, N. T. Son, E. Janzen, N. Morishita, T. Ohshima, H. Itoh, and A. Gali, Phys. Rev. B **71**, 193202 (2005).
[3] N. Mizuochi, S. Yamasaki, H. Takizawa, N. Morishita, T. Ohshima, H. Itoh, and J. Isoya, Phys. Rev. B **68**, 165206 (2003).
[4] N. T. Son, P. Carlsson, J. ul Hassan, E. Janzén, T. Umeda, J. Isoya, A. Gali, M. Bockstedte, N. Morishita, T. Ohsima, and H. Itoh, Phys. Rev. Lett. **96**, 055501 (2006).
[5] T. Umeda, N. T. Son, J. Isoya, E. Janzén, T. Ohshima, N. Morishita, H. Itoh, A. Gali, and M. Bockstedte, Phys. Rev. Lett. **96**, 145501 (2006).
[6] T. Umeda, N. Morishita, T. Ohshima, H. Itoh, and J. Isoya, Mater. Sci. Forum **556-557**, 453 (2007).
[7] N. Mizuochi, S. Yamasaki, H. Takizawa, N. Morishita, T. Ohshima, H. Itoh, T. Umeda, and J. Isoya, Phys. Rev. B **72**, 235208 (2005).
[8] M. Bockstedte, A. Mattausch, and O. Pankratov, Phys. Rev. B **68**, 205201 (2003).
[9] N. T. Son, P. Carlsson, J. ul Hassan, B. Magnusson, and E. Janzén, Phys. Rev. B **75**, 155204 (2007).
[10] A. Gali, N. T. Son, and E. Janzén, Phys. Rev. B **73**, 033204 (2006).
[11] U. Grossner, G. Alfieri, E. V. Monakhov, B. G. Svensson, J. Grillenberger, J. W. Steeds, and W. Sullivan (unpublished).
[12] A. Mattausch, M. Bockstedte, and O. Pankratov, Phys. Rev. B **70**, 235211 (2004).
[13] A. Gali, P. Deak, P. Ordejon, N. T. Son, E. Janzén, and W. J. Choyke, Phys. Rev. B **68**, 125201 (2003).
[14] J. W. Steeds, W. Sullivan, S. A. Furkert, G. A. Evans, and P. J. Wellman, Phys. Rev. B **77**, 195203 (2008).
[15] K. V. Vassilevski, A. B. Horsfall, C. M. Johnson, and N. G. Wright, Mater. Sci. Forum **457-460**, 989 (2004).

[16] J. W. Steeds, S. A. Furkert, W. Sullivan, and G. Wagner, Mater. Sci. Forum **527-529**, 473 (2006).
[17] J. W. Steeds, S. A. Furkert, W. Sullivan, J. M. Hayes, and N. G. Wright, Mater. Sci. Forum **483-485**, 347 (2005).
[18] T. Egilsson, A. Henry, I. G. Ivanov, J. L. Lindström, and E. Janzén, Phys. Rev. B **59**, 8008 (1999).
[19] M. Wagner, B. Magnusson, W. M. Chen, E. Janzén, E. Sörman, C. Hallin, and J. L. Lindström, Phys. Rev. B **62**, 16555 (2000).
[20] T. A. G. Eberlein, R. Jones, S. Öberg, and P. R. Briddon, Phys. Rev. B **74**, 144106 (2006).
[21] A. Mattausch, M. Bockstedte, O. Pankratov, J. W. Steeds, S. Furkert, J. M. Hayes, W. Sullivan, and N. G. Wright, Phys. Rev. B **73**, 161201(R) (2006).
[22] G. A. Evans, J. W. Steeds, L. Ley, M. Hundhausen, N. Schulze, and G. Pensl, Phys. Rev. B **66**, 035204 (2002).
[23] A. Mattausch (private communication).
[24] A. Mattausch, M. Bockstedte, and O. Pankratov, Phys. Rev. B **69**, 045322 (2004).
[25] I. Pintilie, U. Grossner, B. G. Svensson, K. Irmscher, and B. Thomas, Appl. Phys. Lett. **90**, 062113 (2007).